FACTA UNIVERSITATIS
Series: **Physics, Chemistry and Technology** Vol. 13, N° 1, 2015, pp. 13 - 27
DOI: 10.2298/FUPCT1501013P

PHYSICO-CHEMICAL PROCESSES IN VERTICAL-DOUBLE-DIFFUSED METAL-OXIDE-SEMICONDUCTOR FIELD EFFECT TRANSISTORS INDUCED BY GAMMA-RAY IRRADIATION AND POST-IRRADIATION ANNEALING

UDC 621.039 : 541.15

Milić M. Pejović

University of Niš, Faculty of Electronic Engineering, Niš, Serbia

Abstract. *The behavior of commercial power Vertical-Double-Diffused Metal Oxide Semiconductor Field Effect Transistors (VDMOSFETs) during gamma-ray irradiation and subsequent annealing at room and elevated temperature was investigated. The densities of radiation-induced fixed traps and switching traps were determined from the sub-threshold* I-V *curves using the midgap technique. It was shown that the creation of fixed traps dominated during irradiation. The experimental results have also proved the existence of latent switching traps buildup process during annealing at an elevated temperature. This increase correlated with the decrease in fixed trap density. Physical and chemical processes responsible for the threshold voltage shift during irradiation have been analyzed on the basis of interactions between secondary electrons released by gamma photons with covalent bonds* $\mathrm{Si_o - O}$ *and* $\mathrm{Si_o - Si_o}$. *H-W model has been used for the explanation of processes leading to latent switching traps buildup at an elevated temperature and its passivation at late annealing times***.**

Key words: *fixed traps, gamma ray, switching traps, threshold voltage, VDMOS transistor.*

1. INTRODUCTION

Due to their fast switching speed, low noise, simplified input drive requirements and freedom from thermal instabilities, VDMOSFETs are attractive for use in high-frequency, low volume switch power supplies (Baliga, 1981; Sing et al., 1987; Grant and Gowar, 1989). However, during exposure to ionizing radiation electrical characteristics of power VDMOSFET are deleteriously altered, which can limit their utilization in radiation environments, like space (Fleetwood et al., 1991; Gussenhoven, 1996). In order to

Received September 30th, 2014; revised December 1st, 2014; accepted December 15th, 2014.
Corresponding author. Milić M. Pejović
University of Niš, Faculty of Electronic Engineering, Aleksandra Medvedeva 14, 18000 Niš, Serbia
Phone: +38118529324 • E-mail: milic.pejovic@elfak.ni.ac.rs

improve the fabrication technology and thereby achieve greater radiation susceptibility, mechanisms underlying charges in device characteristics need to be elucidated.

In general, ionizing radiation exposure of VDMOSFETs results in a build-up of positive trapped charge in the oxide and an increase in interface-trap density at the SiO_2/Si interface (Ma and Drensserdorfer, 1989). This causes the degradation of several important electrical parameters, such as threshold voltage V_T, transconductance, leakage current and breakdown voltage (Baliga, 1981; Ma and Drensserdorfer, 1989; Singh et al., 1986; Schwank et al., 1992; Oldham et al., 1986). Threshold voltage shift is undoubtedly the most serious problem in power VDMOSFETs. The positive trapped charge in the oxide and interface-trap densities contributes to the threshold voltage shift in the same direction as in p-channel VDMOSFETs, i.e. both induce negative threshold voltage shift (Ma and Drensserdorfer, 1989; Singh et al., 1986). Also, the so-called "rebound effect" (Ma and Drensserdorfer, 1989) is absent in p-channel VDMOSFETs. This phenomenon occurs due to competitive effects of the positive trapped charge in the oxide and negative interface-trap density generated in n-channel VDMOSFETs.

During post-irradiation annealing, the positive trapped charge in the oxide is typically found to be neutralized (Ma and Dresserdorfer, 1989; Schwank, 1992; Oldham et al., 1986; McWhorter et al., 1990; Pejovic et al., 1997; Pejovic and Ristic, 1997, Jaksic et al., 1998a, Pejovic et al., 1998), while the properties of interface traps are more complex. Their density may be unchanged (Schwank et al., 1992a), increased (Schwank et al., 1992a, b) or decreased (Singh et al., 1987). Moreover, some investigations (Fleetwood, 1992; Pejovic et al., 1997) have shown that during annealing an initial increase in interface-trap density may be followed by a decrease at subsequent annealing times. The most intriguing aspect of this investigation is the so-called "latent" interface-trap generation (Schwank et al., 1992a) (a buildup of interface traps during annealing, after an apparent saturation of interface-trap density immediately after irradiation). Namely, (Schwank et al., 1992a, b) was first to observe the latent interface-trap buildup in Si-gate n and p-channel conventional MOSFETs. A similar effect was observed in n-channel VDMOSFETs (Pejovic et al., 1997a; Pejovic et al., 1998) and n-channel conventional MOSFETs (Pejovic et al., 1997b), followed by predominant passivation of interface traps at latter annealing times.

2. EXPERIMENT

2.1. Experimental samples, radiation and annealing

The devices used in these experiments were commercial p-channel power VDMOSFETs, IRF9520 manufactured by International Rectifier. According to the manufacturer's datasheet, breakdown voltage between drain and source V_{DSS} was 100 V, resistance R_{DSon} is 0.6 Ω and maximum drain current at room temperature is 6.8 A. Our measurements have confirmed the above mentioned values from the datasheet. Also, the transistor IRF9520 consists of 1650 cells and its gate oxide thickness is 100 nm (Park and Wie, 2001; Park et al., 2002). Threshold voltage was about 3.5 V and oxide breakdown voltage is about 70 V. IRF9520 is manufactured in standard Si-gate technology with hexagonal cells geometry. Figure 1 presents the layout and cross-section of two cells of this transistor.

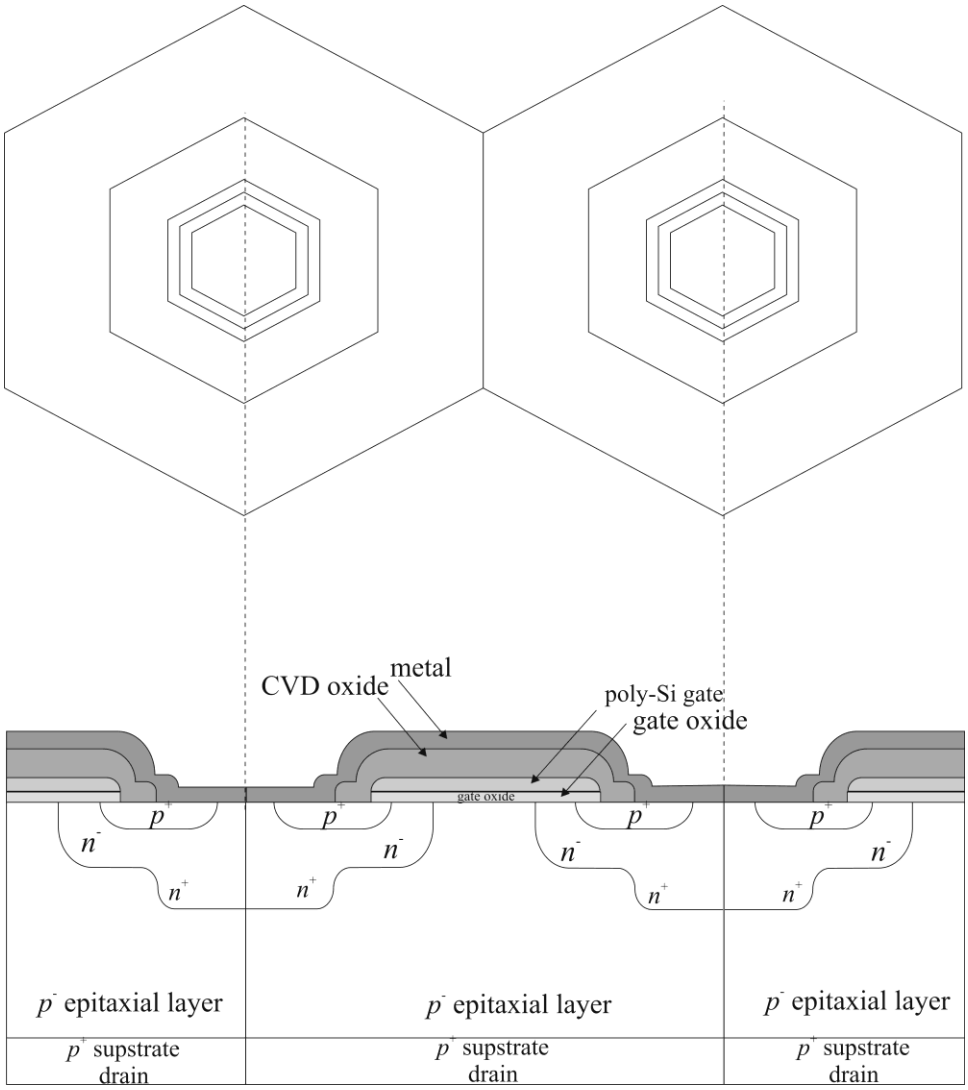

Fig. 1 Two cells layout and cross section of p-channel VDMOSFET.

The transistors were irradiated with gamma-rays from $^{60}_{27}Co$ source at a dose rate of 0.03 Gy(Si)/s to a total dose of 500 Gy. Irradiation source used was a teletherapy cobalt CIRUS-TS source (CIS Alcyon Biointernational, France) with 230 TBq activity (Sept. 1st, 1999). Irradiation was performed in the Secondary Standard Dosimetry Laboratory of the Vinča Institute of Nuclear Science, Vinča, Belgrade, Serbia. All of the measurements were conducted in a climate-controlled laboratory environment at ambient temperature of 20 $\pm$ 0.2 °C. The air kerma rate at reference point was measured with a calibrated vented 0.6 cm^3 ionized chamber Model 30012 and electrometer Unidos (both from PTW Freiburg,

Germany). The calibration of the reference chamber in terms of air kerma was performed at the Secondary Standard Dosimetry Laboratory of the International Atomic Energy Agency (Vienna, Austria). The calibration constants thus obtained was BIPM (Bureau International des Poids et Mesures). A detail uncertainty analysis was performed. Various factors that influence the total air kerma uncertainty were considered. The sources of uncertainty described using statistical estimates are designated as Type A. All other uncertainty estimates are described as Type B. These are subjective estimates based on extensive experience. The factors taken into account are: uncertainty of reference standard, long term stability reference standard, air density (pressure and temperature), positioning of the reference standard, chamber stability, electrometer reading and gamma-ray beam quality. The type A and type B estimates are combined to give an expanded uncertainty (k = 2) which corresponds to the significance of a 95 % confidence level. The expanded and combined uncertainty of air kerma measurements is estimated to be 1.8 %. The air kerma levels were converted in absorbed doses for Si. The gate bias during irradiation was $V_{\text{irr}} = 10\,\text{V}$. After irradiation, the samples were annealed at room temperature for 70000 min without gate bias (all pins were grounded). After that, the annealing process was continued at the 150 °C with gate bias $V_{\text{ann}} = 10\,\text{V}$ for 70000 min using HERAEUS HEP2 system with temperature stability, 150 ^{o}C ± 0.5 °C.

Transistors sub-threshold and transfer characteristics in saturation were measured at room temperature. Equipment used for electrical characterization was Keithley model 4200 SCS (Semiconductor Characterization System). The system is equipped with three medium power source measuring units used for *I-V* characterization. Source measuring units have four voltage ranges: 200 mV, 2 V, 20 V and 200 V, while the current ranges are 100 nA, 1 μA, 10 μA, 100 μA, 1 mA, 10 mA and 100 mA. One of the source measuring units is equipped with pre-amplifier which provides measurements of extremely low currents (0.1 pA). Uncertainty of applied voltage during measurements was 0.015%. The uncertainty of current measurement in the range from 100 μA to 100 mA ranged from 0.033% to 0.045%. On the basis of these data, it can be concluded that threshold voltage was determined with sufficient accuracy.

2.2. Mid-gap-sub-threshold method

The midgap-subthreshold (MG) technique (McWhorter and Winokur, 1986) for determination of traps densities created in the gate oxide (fixed traps) (FT) and near as well as at SiO_2/Si interface (switching traps) (ST) was used. This method is based on FT influences on the carriers in the channel by electrical field and do not have the ability to capture them. The ST created in the oxide near SiO_2/Si interface are called slow switching traps (SST), however the ST created at the SiO_2/Si interface are called fast switching traps (FST) or true interface traps. The ST captures the carriers from the channel in the time framework of the subthreshold/transfer characteristics measurement and their influence on the channel carriers by the electric field can be neglected. In this way, the influence of FT and ST on the transistor subthreshold characteristics is manifested through the parallel shift and its slope variation, respectively.

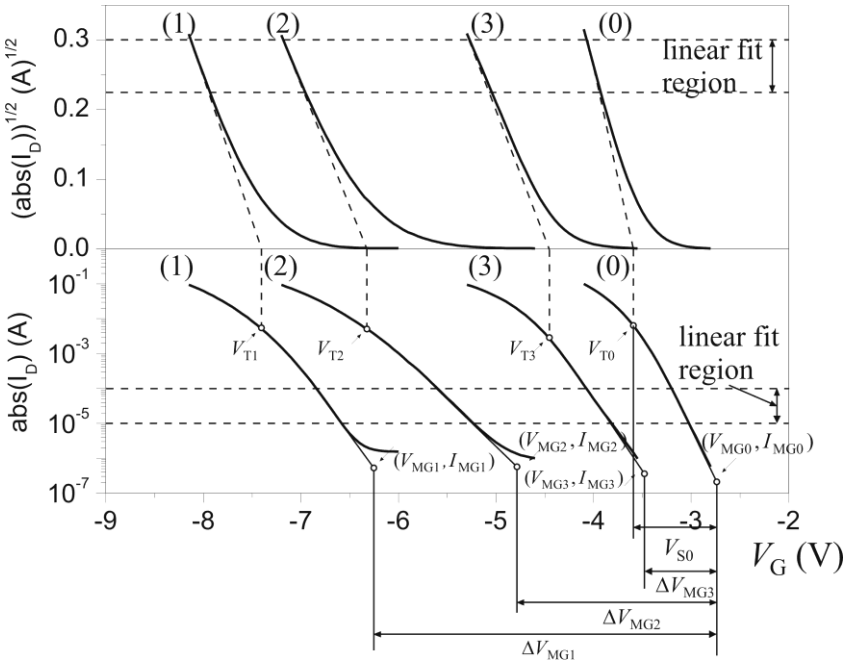

Fig. 2 Transfer characteristics in saturation $(I_D)^{1/2} = f(V_G)$ and subthreshold characteristics $I_D = f(V_G)$: (0)- before irradiation, (1) after 500 Gy irradiation, (2) after annealing at 150°C for t = 15 min and (3) after annealing at 150°C for t = 70000 min.

The MG technique is based on the analysis of MOSFETs subthreshold characteristics (McWhorter and Winokur, 1986). The first step is linear regression of the linear regions of subthreshold characteristics (see Figure 2). The linear regression gives a straight line $\log(I_D) = m \cdot V_G + n$. The next step in the procedure is the calculation of the midgap current before irradiation, I_{MG0}, and after irradiation or annealing I_{MG} (these are the currents $I_{MG1}, I_{MG2}, I_{MG3}$ in Figure 2). The calculation of the midgap current is performed using the subthreshold-current equation for a transistor in saturation (Sze, 1981)

$$I_D = \frac{\sqrt{2}\beta\varepsilon_s}{2C_{ox}L_D} \cdot \left(\frac{kTn_i}{qN_{A,D}} \right)^2 \cdot \sqrt{\frac{q}{kT}\Psi_s} \cdot e^{\frac{q}{kT}\Psi_s}, \quad (1)$$

where $\beta = W\mu C_{ox}/L_{eff}$ and $L_D = \sqrt{\varepsilon_s kT/(q^2 N_{A,D})}$ is the Debye length. In this equation C_{ox} is the oxide capacitance per unit area, k is the Boltzmann's constant, q is the absolute value of electron charge, T is the absolute temperature, n_i is the intrinsic carriers concentration, $N_{A,D}$ is the doping concentration, ε_s is the silicon permittivity, Ψ_s is the surface potential, μ is the carriers mobility, W is the channel width and L_{eff} is the effective channel length. Figure 2 presents subthreshold characteristics for un-irradiated VDMOSFET (curve 0), after 500 Gy irradiation (curve 1), after annealing at 150 °C for the time t = 150 min (curve 2) and after annealing at 150 °C for the time t = 70000 min (curve (3)).

Regardless of the distribution within the substrate energy gap, interface traps are electrically neutral (total charge equals zero) when surface potential Ψ_s is equal to Fermi's potential φ_F, and that is the case when Fermi's level is in the middle of the semiconductor's energy gap. In that case, the shift between two subthreshold characteristics toward the V_G-axis is a consequence of the change of FT only, and the gate voltage which correspond to these surface potential is denoted as V_{MG} (midgap voltage) and it can be obtained as abscissa of the (V_{MG}, I_{MG}) point at the subthreshold characteristics (Figure 2).

Using the strait line equation, $\log(I_D) = m \cdot V_G + n$, V_{MG} can be found as $V_{MG} = [\log(I_{MG}) - n]/m$. Using this procedure V_{MG0}, V_{MG1}, V_{MG2} and V_{MG3} can be found (Figure 2).

The component of threshold voltage shift due to FT, ΔV_{ft}, is

$$\Delta V_{ft} \equiv \Delta V_{MG} = V_{MG} - V_{MG0}, \tag{2}$$

where V_{MG0} and V_{MG} are midgap voltages before irradiation and after irradiation or annealing respectively.

The component of threshold voltage shift due to ST, ΔV_{st}, is

$$\Delta V_{st} = (V_T - V_{MG}) - (V_{T0} - V_{MG0}) = V_S - V_{S0}, \tag{3}$$

where V_{T0} and V_T are transistors threshold voltages before irradiation and after irradiation or annealing, respectively.

V_{T0} and V_T are determined from the transfer characteristics in saturation as the intersection between V_G-axis and extrapolated linear region of $\sqrt{I_D} = f(V_G)$ curves that are modeled by the following equation (Sze, 1981)

$$I_D = \frac{\mu W C_{ox}}{2L_{eff}} (V_G - V_T)^2 . \tag{4}$$

The transistor transfer characteristics in saturation before irradiation (curve 0), after irradiation (curve (1)), after annealing at 150 °C for the time t = 150 min (curve (2)) and after annealing at 150 °C for the time t = 70000 min (curve (3)) are presented in Figure 2. The determination of V_{T0},V_{T1},V_{T2} and V_{T3} is also presented in Figure 2.

The total value of threshold voltage shift, ΔV_T, can be expressed as:

$$\Delta V_T = \Delta V_{ft} + \Delta V_{st} . \tag{5}$$

The areal densities of FT, ΔN_{ft} and ST, ΔN_{st} of irradiated or annealed p-channel MOSFETs can be further determined as (Cartier, 1998; Picard et al., 2000):

$$\Delta N_{ft} = \frac{C_{ox}}{q} \Delta V_{ft}, \; \Delta N_{st} = \frac{C_{ox}}{q} \Delta V_{st} . \tag{6}$$

3. EXPERIMENTAL RESULTS

Figure 3a represents threshold voltage shift ΔV_T as a function of radiation dose D. The symbols in the figure represent $\Delta V_T = V_T - V_{T0}$ values obtained by extrapolation of the

linear region of transfer characteristic in saturation as shown in Figure 2. As it can be seen, the increase of radiation dose up to 500 Gy leads to the increase of ΔV_T for about 4 V. Approximately linear dependence between ΔV_T and D can be also seen from the Figure 3a. Namely, $\Delta V_T = f(D)$ can be described as $\Delta V_T = A \cdot D^n$, where A is the constant and n is the linearity degree. For $n = 1$, the constant A represents the sensitivity which can be expressed as $\Delta V_T / D$. The fitting of experimental data in Figure 3a for $n = 1$ gives the correlation coefficient $r^2 = 0.99$. It can be concluded that there is linear response of VDMOSFET to irradiation doses from 0 to 500 Gy. Such behavior of VDMOSFETs proves the possibility for their application as a sensor in high doses gamma irradiation measurements.

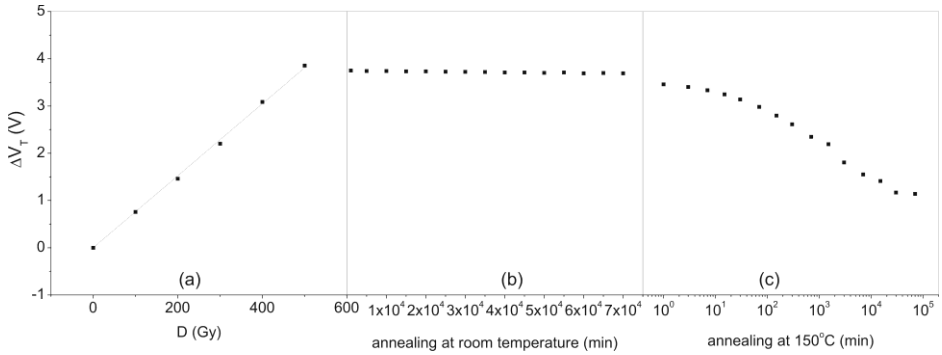

Fig. 3 Threshold voltage shift, ΔV_T during: (a) irradiation, (b) annealing at room temperature and (c) annealing at 150 °C.

The variations in areal density of FT, ΔN_{ft}, are presented in Figure 4a. As expected, the increase in radiation dose, D, lead to the increase in ΔN_{ft}. For radiation dose of 500 Gy, the increase in FT areal density is about $5 \cdot 10^{11}\,\mathrm{cm}^{-2}$. The increase in ST areal density, ΔN_{st}, for the same radiation dose interval is about $1.2 \cdot 10^{10}\,\mathrm{cm}^{-2}$ (Figure 5a).

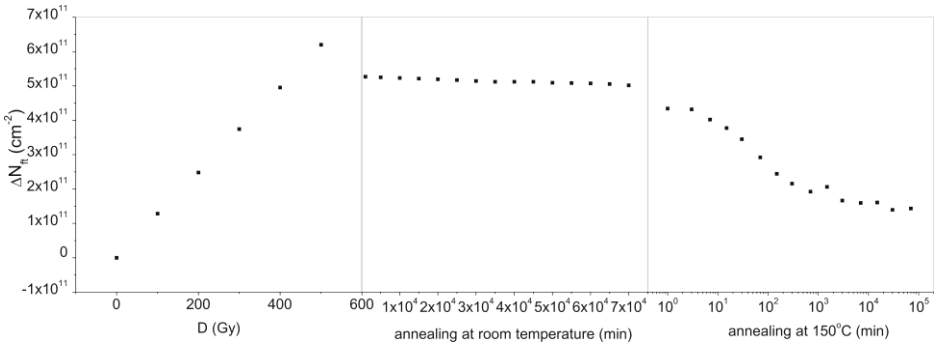

Fig. 4 Areal density of fixed traps, ΔN_{ft} during: (a) irradiation, (b) annealing at room temperature and (c) annealing at 150 °C.

During annealing at room temperature (spontaneous recovery) ΔV_T insignificantly changes (Figure 3b). This is a consequence of insignificant variations in FT and ST

densities. Further annealing of VDMOSFETs at 150 °C with the gate bias of +10 V (Figure 3c) leads to the decrease of threshold voltage shift up to t = 30000 min, and after that further annealing does not influence on the ΔV_T value.

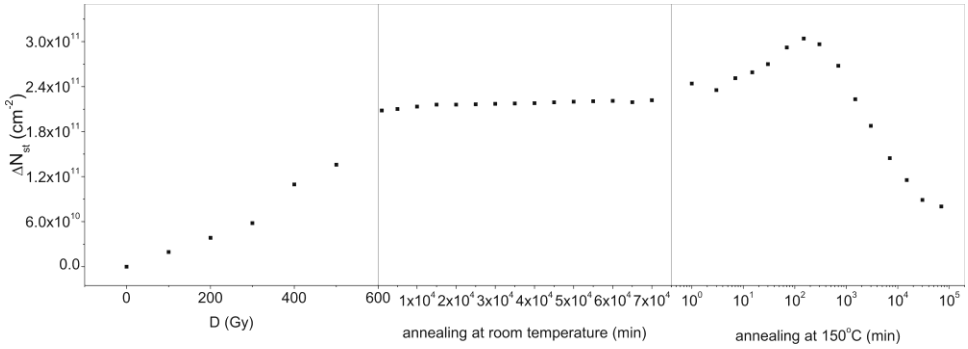

Fig. 5 Areal density of switching traps, ΔN_{st} during: (a) irradiation, (b) annealing at room temperature and (c) annealing at 150 °C.

The variations in FT density during annealing at room temperature and at 150 °C are presented in Figures 4b and 4c, respectively. It can be seen that the annealing at room temperature (Figure 4b) lead to significant decrease in ΔN_{ft} at the beginning of annealing, and in further annealing such decrease is insignificant. The continuation of annealing at 150 °C (Figure 4c) also leads to relatively small decrease in ΔN_{ft} at the beginning. A considerable decrease in ΔN_{ft} during annealing at elevated temperature appears for time interval from 3 to 150 min. After that the decrease is smaller and for t > 30000 min, ΔN_{ft} remains approximately constant.

The variations of ST density during annealing at room and elevated temperature are presented in Figures 5b and 5c, respectively. As it can be seen from Figure 5b, at the beginning of annealing at room temperature there is a significant increase in ΔN_{st}. At further annealing at room temperature and at the beginning of annealing at 150 °C (Figure 5c) ΔN_{st} insignificantly changes. Annealing at elevated temperature for the period of 3 to 150 min leads to a sudden increase of ΔN_{ft} values. From 150 to 30000 min, ΔN_{st} significantly decreases and for t > 30000 min ΔN_{st} remains approximately constant. On the basis on ΔN_{ft} and ΔN_{st} behavior during annealing at room temperature (Figures 4b and 5b) it can be concluded why the ΔV_T ΔV_T remains constant (Figure 3b).

4. DISCUSSION

During irradiation gamma photons interact with the electrons in SiO_2 molecules mainly via Compton's scattering there for releasing secondary electrons and holes. Secondary electrons, which are highly energetic, may be recombined with holes at the place of production, or may escape recombination. Secondary electrons that escape recombination with holes travel some distance until they leave the oxide, losing kinetic energy through the

collision with the bonded electrons in $Si_o - O$ and $Si_o - Si_o$ covalent bonds in the oxide (the latter bond represents an oxygen vacancy) and further releasing more electrons.

Each secondary electron, before it leaves the oxide or is recombined by a hole, can break a lot of covalent bonds in the oxide, thus producing a lot of new secondary highly energetic electrons, since its energy is usually much higher than an impact ionization process energy (an energy of 18 eV is necessary for the creation of one electron-hole pair (Ma and Dresserdorfer, 1989), i.e. for the electron ionization). It is obvious that the secondary electrons play a more important role in bond breaking than highly energetic photons, as a consequence of the difference in their effective masses, i.e. in their effective cross section. The electrons leaving the place of formation escape from the oxide very fast (several picoseconds), while the holes remain in the oxide.

The holes released in the oxide bulk move toward one of the interfaces (SiO_2/Si or gate SiO_2) depending on the oxide electric field direction, where they will be trapped at energetically deeper trap hole centers. Since the gate bias in our experiments was +10 V the electric field direction was directing the holes toward SiO_2/Si interface.

A secondary electrons passing through the oxide bulk collides with a bonded electron in the non-strained silicon-oxygen bond, $\equiv Si_o - O - Si_o \equiv$ (it could also be represented as $\equiv Si_o^{\bullet\bullet} O^{\bullet\bullet} Si_o \equiv$ where $^{\bullet\bullet}$ represents two electrons making a covalent bond), by the reactions (Ristic, 2008)

$$\equiv Si_o - O - Si_o \equiv \xrightarrow{e^-} \equiv Si_o - O^{\bullet} + {}^{+}Si_o \equiv 2e^- , \tag{7}$$

$$\equiv Si_o - O - Si_o \equiv \xrightarrow{e^-} \equiv Si_o - O^{+} + {}^{\bullet}Si_o \equiv 2e^- , \tag{8}$$

where $\equiv$, the indexes $_o$ and $^{\bullet}$ denote the three $Si_o - O$ bonds ($O_3 \equiv Si_o - O$), silicon atom in the oxide and electron, respectively. Reaction (7) is much more probable in the oxide bulk, since these are the most numerous centers. The formed $Si_o - O^{\bullet +} Si_o \equiv$ complex is energetically very shallow, representing the temporary hole center (the trapped holes can easily leave it (Sah, 1976)).

The $\equiv Si_o - O - Si_o \equiv$, which are mainly distributed near SiO_2/Si interface can also easily be broken by the passing of secondary electrons, usually creating amphoteric non-bridging-oxygen (NBO) center, $\equiv Si_o - O^{\bullet}$, and positively charged $E^{'}$ center, $\equiv Si_o^{+}$ (Griscom, 1991) known as $E_s^{'}$ center (Helms and Poindexter, 1994) (processes shown in reaction (7)). An NBO center is an amphoteric defect that could be easily negatively charged than positively charged by trapping an electron:

$$\equiv Si_o - O^{\bullet} + e^- \rightarrow \equiv Si_o - O^- . \tag{9}$$

Obviously, the NBO center, as an energetically deeper center, is the main precursor of the negatively charged traps (defects) in the oxide bulk and near the SiO_2/Si interface region.

A secondary electron passing through the oxide can also collide with an electron in the strained oxygen vacancy bond $\equiv Si_o - Si_o \equiv$, i.e. $\equiv Si_o^{\bullet\bullet} Si_o \equiv$, which is a precursor of an $E_{\gamma}^{'}$ center ($\equiv Si_o^{\bullet}$) (Weeks, 1956), breaking this bond and knocking out an electron (Nenoi, 2012)

$$\equiv Si_o^{\bullet\bullet} Si_o \equiv \xrightarrow{e^-} \equiv Si_o^{+} + {}^{\bullet} Si_o \equiv +2e^- . \tag{10}$$

Else, this is a conventional structural model of the $E_{\gamma}^{'}$ center: a hole trapped at an oxygen mono-vacancy ($\equiv Si_o^{+\bullet}Si_o \equiv$). The oxygen vacancy bonds are mainly distributed in the vicinity of the interface.

The reactions (7), (8) and (10) could occur everywhere in the oxide: near the interfaces and in the oxide bulk. The trapped charge can be positive (oxide trapped holes) and negative (oxide trapped electrons), and the former is more important, since the hole trapping centers are more numerous, including $E_s^{'}$, $E_{\gamma}^{'}$ and NBO centers, compared to one electron NBO trap center.

The holes trapped at $\equiv Si_o^{+}$ centers formed from the oxygen vacancies and strained silicon-oxygen bonds are energetically deep and steady, and the holes can remain in them for a long time period, i.e. they can hardly be filled by electrons compared to some shallowly trapped holes. These centers exist especially near the SiO_2/Si interface. The holes created and trapped at the bulk defects (reaction (7)), representing energetically shallow centers, are forced to move towards SiO_2/Si interface under the positive electric field, where they are trapped at deeper traps, since there are a lot of oxygen vacancies, as well as a lot of strained silicon-oxygen bonds near the interfaces, grouping all of the positive trapped charge there. The holes leave the energetically shallow centers in the oxide transported to the interface by a hopping process using either shallow centers in the oxide (Boech, 1975). When the holes reach the interface, they can break both the strained silicon-oxygen bonds $\equiv Si_o - O - Si_o \equiv$, forming the amphoteric NBO centers $\equiv Si_o - O^{\bullet}$ and $E_s^{'}$ centers $\equiv Si_o^{+}$ (Griscom, 1991):

$$\equiv Si_o - O - Si_o \equiv + h^{+} \rightarrow \equiv Si_o - O^{\bullet} + \equiv Si_o^{+} \tag{11}$$

and the strained oxygen vacancy bonds $\equiv Si_o\text{-}Si_o \equiv$, forming $E_{\gamma}^{'}$ centers $\equiv Si_o^{\bullet}$

$$\equiv Si_o - Si_o \equiv + h^{+} \rightarrow \equiv Si_o^{\bullet} + \equiv Si_o^{+} \tag{12}$$

It should be emphasized that the strained silicon-oxygen bonds $\equiv Si_o - O - Si_o \equiv$ and the oxygen vacancy $\equiv Si_o\text{-}Si_o \equiv$ represent the main defect precursor in the oxide bulk and near the SiO_2/Si interface. It could be assumed that these defects represent FT and SST (Ristic et al., 2006). They can be positively or negatively charged, as well as neutral.

Moving through the oxide, the holes can also react with hydrogen defect precursors such as $\equiv Si_o - H$ and $\equiv Si_o - OH$, creating following defects (Jaksic et al., 1996b):

$$\equiv Si_o - H + h^{+} \rightarrow \equiv Si_o^{\bullet} + H^{+}, \tag{13}$$

$$\equiv Si_o - H + h^{+} \rightarrow \equiv Si_o^{+} + H^{o}, \tag{14}$$

$$\equiv Si_o - OH + h^{+} \rightarrow \equiv Si_o - O^{\bullet} + H^{+}, \tag{15}$$

$$\equiv Si_o - OH + h^{+} \rightarrow \equiv Si_o - O^{+} + H^{o}. \tag{16}$$

The precursors given in these reactions are only important for the holes that transport through the oxide since the hydrogen is relatively weakly bonded, and the holes can easily break these bonds.

The defects at the SiO_2/Si interface known as FST, true interface traps or P_b center represent an amphoteric defect $Si_3 \equiv Si_s^{\bullet}$: a silicon atom $\equiv Si_s^{\bullet}$ at the SiO_2/Si interface

back bonded to three silicon atoms from the substrate $\equiv Si_3$, and are usually denoted as $\equiv Si_s^{\bullet}$ or $Si_s^{\bullet}$. FST can be created by trapped holes (h^+ model) (Lai, 1983; Chang et al., 1986; Wang et al., 1988). Namely, when holes are trapped near the interface and electrons are subsequently injected from the substrate and recombination occurs. From the energy released by electron-hole recombination an interface state may be formed. Although a reaction for the FST creation has not been given, it could be emphasized as (Ristic, 2008)

$$\equiv Si_o^+ + e^- + \equiv Si_s - Si_s \equiv \rightarrow \equiv Si_o^{\bullet} + \equiv Si_s^{\bullet}. \quad (17)$$

The main lack of the h^+ model is its impossibility in explaining the delayed creation of FST (Saks and Brown, 1989).

FST are also created by hydrogen released in the oxide (hydrogen-related species model-H model) (Saks and Brown, 1989; McLean, 1980; Saks at al., 1988). H^+ ions, released in oxide by trapped holes (reactions (13) and (15)) drift towards the SiO_2/Si interface under the positive electric field (the case used in these investigations). When the H^+ ion arrives at the interface, it picks up an electron from the substrate, becoming a highly reactive atom H^o (Griscom et al., 1988)

$$H^+ + e^- (\text{from the substrate}) \rightarrow H^o. \quad (18)$$

Also, according to the H model, the hydrogen atoms H^o, released by reactions (14) and (16), diffuse towards SiO_2/Si interface under the existing concentration gradient.

The creation of $Si_s^{\bullet}$ (FST) when H^o reacts with an interface precursor $Si_s - H$ (Griscom et al., 1988):

$$Si_s - H + H^o \rightarrow Si_s^{\bullet} + H_2, \quad (19)$$

or an interface trap precursor $Si_s - OH$:

$$Si_s - OH + H^o \rightarrow Si_s^{\bullet} + H_2O \quad (20)$$

producing FST.

With the increase in radiation dose FT, SST and FST (ST = SST + FST) density increases in the oxide and at SiO_2/Si interface (Figures 4a and 5a), which further leads to the increase in threshold voltage shift, ΔV_T (Figure 3a).

The h^+ model and H-model are not successful in explanation of two important aspects of the data presented in Section 3: (1) the fact that the FST buildup is still going on after very long annealing at room temperature and at beginning at 150 °C and (2) the fact that the FST buildup is followed by a their passivation at latter annealing times (see Figures 4c and 5c). Namely, since the drift of holes through the oxide is a fast process (it takes less than 1 s for all radiation-induced holes to reach the SiO_2/Si interface (Ma and Dresserdorfer, 1989, Saks et al., 1988)), the trapped-hole model can explain only the second order effect-"prompt" interface-traps generation (Oldham et al., 1989). Although, the drift of H^+ ions, which is the rate limiting step for the ST generation in hydrogen ion transport models, is much slower than the drift of holes, it is still very far from accounting for the time scale needed for FST build-up in our experiments (it takes only a few hours at room temperature (Saks et al., 1989) and a few seconds at elevated temperature for all

radiation-induced H^+ ions to reach the SiO_2/Si interface). Moreover, after consuming all of the holes/hydrogen ions in the interface-trap formation process, the ΔN_{st} should be expected to saturate, which is not always the case (Pejovic and Ristic, 1997; Pejovic et al., 1998; Fleetwood, 1992). Because of that, the hydrogen-water model was proposed (H-W model) (Pejovic et al., 1997a; Pejovic and Ristic, 1997; Pejovic et al., 1998). This model uses hydrogen ion transport as a foundation. Another hydrogenous species - H_2O molecule, was included in explanation of FST kinetics.

As mentioned above, there is a large number of $\equiv Si_o - H$ and $\equiv Si_o - OH$ bonds in the oxide (Jaksic et al., 1996b). Radiation-induced holes which drift toward the SiO_2/Si interface can break these bonds and liberate H^+ ions (reactions (13) and (15)). As the result of irradiation, hydrogen atoms (H) are produced in the oxide (reactions (14) and (16)), and in interaction with holes also lead to the creation of H^+ (Saks et al., 1993):

$$H + h^+ \rightarrow H^+ . \tag{21}$$

Under a positive electric field, H^+ ion drifts toward SiO_2/Si interface and picks up an electron from silicon (reaction (18)) which reacts with interface-trap precursor $\equiv Si_s - H$ and produces an interface trap and molecular hydrogen (reaction (19)).

Besides taking part in reaction (19), atomic hydrogen may dimerize (Griscom, 1985)

$$2H \rightarrow H_2 . \tag{22}$$

As a consequence of reactions (19) and (22), there is an increased concentration of H_2 molecules at the interface, and H_2 diffuses towards the oxide bulk, where it can be cracked at the positive charge centers in the oxide CC^+ (Stahlbush et al., 1993a):

$$CC^+ + H_2 \rightarrow CC - H + H^+ . \tag{23}$$

It is shown (Stahlbush et al., 1993a, b) that the oxygen-related hole traps most readily crack H_2. However, there is evidence that E_s' centers also easily react with H_2 (Conley and Lenahan, 1993), which particularly would be expected at elevated temperatures, as in our case (150 °C). It is also shown (Stahlbush et al., 1993a) that the cracking reaction (23) is the rate limiting step in interface-trap formation. The H^+ produced in reaction (23) drifts toward the SiO_2/Si interface and the reaction sequence (18), (19), (22) and (23) takes place repeatedly. This reaction sequence ensures the source of H^+ ions during a very long period of annealing time which lead to a very long time scale of FST buildup. Reaction (23) is the additional mechanism responsible for FT decrease and explains the correlation between ST buildup and FT charge neutralization.

According to H-W mode, simultaneously with the FST formation, their passivation also takes place. Passivation may be attributed to reactive H^o escaping dimerization in reaction (19) and (22) (Reed and Plummer, 1987; Cartier, 1993) and water molecules which diffuse through the oxide to SiO_2/Si interface (Stahlbush et al., 1998; Brown et al., 1983):

$$\equiv Si_s^{\bullet} + H^o \rightarrow \equiv Si_s - H , \tag{24}$$

$$\equiv Si_s^{\bullet} + H_2O \rightarrow \equiv Si_s - OH + H^o . \quad (25)$$

It can be seen that H^o may either create (reaction (19)) or passivate (reaction (24)) FST. Since both of these reactions have essentially no energy barrier (Cartier 1993), their probabilities depend on the concentrations of the reactant, $\equiv Si_s - H$ and $\equiv Si_s^{\bullet}$. At the beginning of annealing, reaction (19) is predominant, due to the concentration of interface-trap precursors and the smaller concentration of FST. At late annealing times, as the concentration of interface-traps precursors decreases and FST increases, the probability for reaction (19) decreases and the probability for reaction (24) is increased. At some annealing time reactions (19) and (24) comes to a balance, leading to the saturation in ΔN_{st}, but the H_2O molecules, which slowly diffuse through the oxide contribute to the predominant passivation of interface traps at subsequent annealing time via reaction (25).

The net effect of the arrival at the SiO_2/Si interface for one H_2O molecule may not always be the passivation of one interface-trap. Namely, H^o created by reaction (25) may take part in any of reactions (19), (22) and (24). In the first case, there is no change in FST density, but an H_2 molecule is produced. In the second case, H_2O molecule passivates one FST, and in the third case the net effect is passivation of two FST.

Earlier investigations (Pejovic et al., 1997; Pejovic et al., 1998) have shown that H-W model can very successfully describe the FST behavior during irradiated power n-channel VDMOSFETs annealing at elevated temperature. The results presented in this paper proves that H-W model very well describes FT and ST behavior during annealing at elevated temperatures of irradiated commercial p-channel power VDMOSFETs. Namely, there is a correlation between the FT density decrease and the rapid increase in ST density (Figures 4c and 5c). This model also explains the decrease in ST density after long annealing times (Figure 5c).

5. CONCLUSION

During gamma-ray irradiation of VDMOSFETs the most important physical and chemical processes take place in SiO_2 and SiO_2/Si interface. These processes lead to the increase in fixed traps (FT) density in the oxide, i.e. the increase in positive trapped charge in the oxide, which consists of E_s' ($\equiv Si_o^+$), NBO ($\equiv Si_o - O^{\bullet}$) and E_γ' ($\equiv Si_o^{\bullet}$) centers. Switching traps ST density also increases near the SiO_2/Si interface. They consist of slow switching traps SST and they mainly represent E_γ' centers, as well the fast switching traps (FST) or P_b centers (ST = SST + FST). These processes lead to instabilities of VDMOSFETs electrical parameters. The most important one is threshold voltage shift ΔV_T. The results of irradiated VDMOSFETs annealing at 150 ^{o}C show latent buildup of FST along with simultaneous decrease in FT density. At late annealing time, the passivation of FST dominates. Such FST behavior during annealing can be explained by hydrogen-water (H-W) model, which was developed at Faculty of Electronic Engineering in Nis (Pejovic et al., 1998). The H-W model shows that if FT is present in the oxide, than a small concentration of hydrogen molecules (ions) or water molecules, at late annealing is sufficient to trigger the latent build-up of FST. The experimental results have confirmed this, showing a direct relation between FST creation and FT neutralization. This

model is based on the assumption that water molecules are responsible for passivation process of FST at late annealing times of irradiated p-channel VDMOSFET. Finally, from the proposed mechanisms, it can be concluded that latent FST buildup can be minimized by fabrication process variations which can reduce the amount of hydrogen in the gate oxide. However, because the hydrogen plays a positive role in reduction of process-induced (pre-irradiation) FST, an acceptable compromise has to be made between pre- and post-irradiation stability of the device.

To conclude, on the basis of linear dependence between threshold voltage shift and radiation dose it can be stated that the VDMOSFET sensitivity is the same throughout the 500 Gy dose range. It shows that these transistors can be very useful as sensor for high gamma radiation doses.

Acknowledgement: *The work presented in this paper has been supported by the Ministry of Education, Science and Technological Development of the Republic of Serbia under the Contract no. 171007.*

REFERENCES

Baliga, B. J., 1981. IEEE Spectrum, 18, 42-48.
Boesh, H. E., McLean, F. B., McGarrity, J. M., Ausman, G. A., 1975. IEEE Trans. Nucl. Sci., 22, 2153-2167.
Brown, D. B., Ma, D. I., Dozier, C. M., Peckerar, M. C., 1983. IEEE Trans. Nucl. Sci., 30, 4059-4063.
Cartier, E., 1998. Microelectron. Reliab., 38, 201-211.
Cartier, E., Stathis, J. H., Buchanan, D. A., 1993. Appl. Phys. Lett., 63, 1510-1512.
Chang, S. T., Wu, J. K., Lyon, S. A., 1986. Appl. Phys. Lett., 48, 662-664.
Conley, J. F., Lenahan, P. M., 1993. Appl. Phys. Lett., 62, 40-42.
Fleetwood, D. M., 1992. Appl. Phys. Lett., 60, 2883-2885.
Fleetwood, D. M., Winokur, P. S., Meisenheimer, T. L., 1991. IEEE Trans. Nucl. Sci., 38, 1552-1556.
Grant, D. A., Gowar, J., 1989. Power MOSFETS-Theory and Application, New York: Willey and Sons.
Griscom, D. L., 1985. J. Appl. Phys., 58, 2524-2533.
Griscom, D. L., Brown, D. B., Saks, N. S., 1988. Nature of radiation-induced point defects in amorphous SiO_2 and their role in SiO_2-on Si structures, The Physics and Chemistry of SiO_2 and the Si-SiO_2 interface, New York: Plenum.
Griscom, D. L., 1991. J. Ceram. Soc. Jpn., 99, 923-941.
Gussenhoven, M. S., Mullen, E. G., Brautigam, D. H., 1996. IEEE Trans. Nucl. Sci., 43, 353-358.
Helms, R., Poindexter, E. H., 1994. Rep. Prog. Phys., 57, 791-852.
Lai, S. K., 1983. J. Appl. Phys., 54, 2540-2546.
Jaksic, A., Ristic, G., Pejovic, M., 1996. Phys. Stat. Sol. (a), 155, 371-379.
Jaksic, A., Pejovic, M., Ristic, G., Rakovic, S., 1998. IEEE Trans. Nucl. Sci., 45, 1365-1371.
Ma, T. P., Drensserdorfer, P. V. Eds., 1989. Ionizing Radiation Effects in MOS Devices and Circuits, New York: Wiley-Interscience.
McLean, F. B., 1980. IEEE Trans. Nucl. Sci., 27, 1651-1657.
McWhorter, P. J., Winokur, P. S., 1986. Appl. Phys. Lett., 48, 1133-1135.
McWhorter, P. J., Miller, S. L., Miller, W. M., 1990. IEEE Trans. Nucl. Sci., 37, 1682-1687.
Nenoi, M., ed., 2012. Current Topic in Ionizing Radiation Research, In Tech., Rijeka, Opatija.
Oldham, T. R., Lelis, A. J., McLean, F. B., 1986. IEEE Trans. Nucl. Sci., 33, 1203-1210.
Oldham, T. R., Boesh, H. E., McLean, F. B., McGarrity, J. M., 1989. Semicond. Sci. Tech., 4, 986-999.
Park, M. S., Wie, C., 2001. IEEE Trans. Nucl. Sci., 48, 2285-2293.
Park, M. S., Na, I., Lee, C., Wie, C., 2002. IEEE Trans. Nucl. Sci., 49, 3230-3237.
Pejovic, M., Ristic, G., Jaksic, A., 1997. Appl. Surf. Sci., 108, 141-148.
Pejovic, M., Ristic, G., 1997. Solid State Electron., 41, 715-720.

Pejovic, M., Jaksic, A., Ristic, G., Baljosevic, B., 1997. Rad. Phys. Chem., 49, 521-525.
Pejovic, M., Jaksic, A., Ristic, G., 1998. J. Non-Cryst. Solids, 240, 182-192.
Picard, P., Brisset, C., Ouittard, O., Hofman, A., Jaffre, F., Charles, J. P., 2000. IEEE Trans. Nucl. Sci., 47, 641-646.
Reed, M. L., Plumer, J., 1987. Appl. Phys. Lett., 51, 514-516.
Reed, M. L., 1987. Si-SiO_2 trap anneal kinetics, Stanford University, PhD. Thesis.
Ristic, G. S., Pejovic, M. M., Jaksic, A. B., 2006. Appl. Surf. Sci., 252, 3023-3032.
Ristic, G., 2008. J. Phys. D: Appl. Phys., 41, 023001 (19).
Saks, N. S., Dozier, C. M., Brown, D. B., 1988. IEEE Trans. Nucl. Sci., 35, 1168-1177.
Saks, N. S., Brown, D. B., 1989. IEEE Trans. Nucl. Sci., 36, 1848-1857.
Saks, N., Klein, R. B., Stuhbush, R. E., Mrstik, B. J., Rendell, R. V., 1993. IEEE Trans. Nucl. Sci., 40, 1341-1345.
Sah, C. T., 1976. IEEE Trans. Nucl. Sci., 23, 1563-1567.
Schwank, J. R., Fleetwood, D. M., Shaneyfelt, M. R., Winokur, P. S., 1992. IEEE Electron Dev. Lett., 13, 203-205.
Schwank, J. R., Fleetwood, D. M., Shaneyfelt, M. R., Winokur, P. S., Axness, C. L., Riewe, L. C., 1992. IEEE Trans. Nucl. Sci., 39, 1953-1963.
Singh, G., Galloway, K. F., Russell, T. J., 1987. IEEE Trans. Nucl. Sci., 34, 1366-1369.
Singh, G., Galloway, K. F., Russel, T. J., 1986. IEEE Trans. Nucl. Sci., 33, 1454-1459.
Stahlbush, R. E., Lawrence, R. K., Huges, H. L., Saks, N. S., 1988. IEEE Trans. Nucl. Sci., 35, 1192-1196.
Stahlbush, R. E., Edwards, A. H., Griscom, D. L., Mrstik, B. J., 1993. J. Appl. Phys., 73, 658-667.
Stahlbush, R. E., Edwards, A. H., 1993. The Physics and Chemistry of Si and SiO_2 Interface 2, Plenum, New York.
Sze, S. M., 1981. Physics of Semiconductor Devices, New York: Wiley.
Wang, S. J., Sung, J. M., Lyon, S. A., 1988. Appl. Phys. Lett., 52, 1431-1433.
Weeks, R. A., 1956. J. Appl. Phys., 27, 1376-1381.

FIZIČKO-HEMIJSKI PROCESI U VDMOSFET-U IZAZVANI GAMA ZRAČENJEM I OPORAVKOM POSLE ZRAČENJA

Istraživano je ponašanje snažnih VDMOSFET-a za vreme ozračivanja gama zračenjem i kasnijeg oporavka na sobnoj i povišenoj temperaturi. Gustine defekata u oksidu i na međupovršini su određivane iz predpragovske karakteristike korišćenjem midgap metode. Eksperimentalni rezultati su potvrdili postojanje latentnog porasta površinskih stanja na Si-SiO_2 međupovršini koji se stvaraju za vreme oporavka na povišenoj temperaturi. Njihov porast je praćen smanjenjem zahvaćenog naelektrisanja u oksidu. Fizičko-hemijski procesi koji dovode do promene napona praga za vreme zračenja su analizirani na osnovu interakcija između sekundarnih elektrona, oslobođenih gama fotonima i kovalentnih Si_o – O i Si_o – Si_o veza. H-W model je korišćen za objašnjenje procesa koji dovode do pojave latentnog porasta površinskih stanja na Si-SiO_2 međupovršini na povišenoj temperaturi kao i njihove pasivizacije tokom kasnijeg oporavka.

Key words: *fiksni centri, gama zračenje, promenljivi centri, napon praga, VDMOS transistor.*